R.B. HNATYK, V.V. VOITSEKHOVSKYI

Astronomical Observatory, Taras Shevchenko National University of Kyiv
(3 Observatorna Str., Kyiv 04053, Ukraine; e-mail: roman.hnatyk@knu.ua)

GAMMA-RAY AND NEUTRINO RADIATION FROM COMA CLUSTER (A1656)

Galaxy clusters (GCs) are the largest and the most massive gravitationally bounded objects in the large-scale structure of the Universe. Due to the high (of the order of a few keV) temperature of virialized gas in the intracluster medium (ICM) and the presence of cosmic rays (CRs), GCs are effective sources of thermal X-ray and non-thermal lepton (synchrotron) radiation. GCs are also storage rooms for CRs because the time of CR diffusive escape from GCs exceeds the age of the Universe. However, non-thermal hadronic gamma-ray emission from GCs, which mainly arises due to proton-proton collisions of CRs and thermal protons of ICM plasma and the subsequent decay of neutral pions, has not yet been robustly detected. In this paper, we model the expected non-thermal hadronic gamma-ray radiation and neutrino flux from the Coma cluster (A1656) and evaluate the prospects for registering this radiation making use of available (Fermi-LAT, LHAASO, IceCube) and planned (CTA, IceCube-Gen2) ground-based detectors.

K e y w o r d s: galaxy clusters, Coma cluster, cosmic rays, gamma radiation, neutrino radiation.

1. Introduction

Galaxy clusters (GCs) are the largest and most massive, mostly virilized structures in the Universe at the current cosmological time $t_0 = 13.8 \times 10^9$ years [1]. The growth of initial density perturbations owing to the gravitational instability leads to the formation of basic elements of large-scale structure such as leaf-like structures confining voids, i.e., areas of a reduced density, and filaments connecting nodes, i.e., galaxy clusters and superclusters [2]. The dominant contribution to the total GC gravitational masses $M_{cl} \sim 10^{14} \div 10^{15}$ M$_\odot$ is made by the dark matter (approximately 80%). A much smaller contribution is made by the baryon matter (about 15% in the gas of intracluster medium (ICM) and about 5% in stars and galaxies) [3–5]. The virial temperature of ICM plasma $k_B T \sim G M_{cl} m_p / R_{cl}$ in a GC with typical dimensions $R_{cl} \sim 2 \div 3$ Mpc equals 1–10 keV. Therefore, GCs are bright sources of thermal X-ray radiation with typical luminosities $L_X \sim 10^{44} \div 10^{46}$ erg/s.

The formation of gravitationally bound and virialized GCs is a long process of halo collapse and merging of substructures that are not yet complete in most cases. Most clusters have not yet fully relaxed, so the accretion and merging processes are still continuing. Magnetohydrodynamic fluxes in the ICM and active galactic nuclei (AGNs) are accompanied by the appearance of multiple shock waves that effectively accelerate cosmic rays (CRs) and amplify or generate a magnetic field. In the magnetic field $B_{cl} \sim 1 \div 10$ μGs, which is typical of GCs, the time of CR diffusive escape from a GC, $t_{diff} \sim R_{cl}^2 / D(E)$, is of the same order of magnitude as or even larger than the age of the Universe provided typical values of the diffusion coefficient, $D(E) \sim 10^{28}(E/10 \text{ GeV})^{0.5}$ cm^2 s^{-1}. As a result, GCs are effective accumulators for accelerated CRs [4]. Hence, GCs should be promising sources of non-thermal lepton (synchrotron) radiation emission, as well as hadronic gamma radiation (mainly via proton-proton collisions and subsequent decays of neutral pions) [6, 7]. Really, non-thermal synchrotron radiation emission is widely represented in GC observational data, but no non-thermal gamma radiation from GCs has been reliably detected yet [8, 9].

Both non-thermal radio emission and thermal X-ray emission data, supplemented with the data from the Planck Observatory concerning the Sunyaev–Zeldovich thermal effect, provide valuable information on the spatial distribution of the baryon and

dark matter, as well as on physical processes running in the ICM of GCs [10]. In this work, we will simulate non-thermal hadronic gamma and neutrino radiation from the GC A1656 (the Coma cluster) and evaluate the prospects of observing this GC making use of available and planned (*Fermi*-LAT, LHAASO, IceCube, CTA, IceCube-Gen2) space missions and ground-based detectors. In calculations, the MINOT software [10] and the ΛCDM cosmological model with the parameters $H_0 = 67.8$ km s^{-1} Mps^{-1}, $\Omega_M = 0.308$, and $\Omega_\Lambda = 0.692$ [11] were used.

2. Coma Cluster

The Coma GC (A1656) has the red shift $z = 0.0231$. Recently, gamma radiation in the A1656 direction has been detected for the first time with the help of the *Fermi*-LAT telescope [12,13]. Both the Coma GC and the *Fermi*-LAT point source 4FGL J1256.9+2736 (radio galaxy NGC 4839) can be its source. Therefore, this GC is a good candidate for the further study of the generation of non-thermal gamma radiation and neutrinos in the harder (TeV) gamma spectral interval. Besides the proton-proton interactions in the ICM, one may expect that the active nucleus of the galaxy NGC 4839 should also make a contribution to the total radiation flux [13]. For instance, the arrival direction of high-energy neutrinos detected by IceCube (event IC200921A) coincides with the AGN of NGC 4839 within a localization error of 90% [14].

Physical conditions and the spherically symmetric distribution of dark/baryon matter in the ICM of GCs are determined by a number of physical parameters, which will be presented below (a detailed description of physical characteristics of clusters can be found in work [10]). In particular, GCs are described by a few characteristic masses that are used while modeling the GC parameters. In particular, the notation M_{500} is applied to denote the mass located within the region of radius R_{500}, where the averaged (over the volume) density is 500 times as high as the critical density, $\rho/\rho_{cr} = 500$. The corresponding quantitiesare related to one another via the following relation:

$$M_{500} = \frac{4\pi}{3} 500 \rho_{cr} R_{500}^3. \qquad (1)$$

The total GC mass M_{tot} is somewhat larger than the mass M_{HSE} calculated from the hydrostatic equilibrium condition, $M_{tot} = M_{HSE}/(1 - b_{HSE})$, which

is taken into account using the correction parameter $b_{HSE} \approx 0.2$ [15, 16]. The spatial distribution of the gas fraction in GCs, $f_{gas}(r)$, is given by the ratio between the total gas mass of gas $M_{gas}(r)$ and the total mass $M_{tot}(r)$ within the sphere of radius r, $f_{gas}(r) = M_{gas}(r)/M_{tot}(r)$.

The profile of the electron gas density, $n_e(r)$, is an important parameter for evaluating gamma radiation because the latter is proportional to the total gas density $n_{gas}(r)$, which is responsible for the intensity of proton-proton interactions. There are a number of theoretical models describing $n_e(r)$. In particular, the semi-analytical beta model [17]

$$n_e(r) = n_{e,0} \left[1 + \left(\frac{r}{r_c}\right)^2\right]^{-3\beta_{dens}/2}, \qquad (2)$$

where $n_{e,0}$ is the normalizing factor, r_c the radius of the central part of distribution, and β_{dens} the density index, will be used in this work.

The thermal gas pressure is another important model parameter because it allows the amount of CRs the energy of which is proportional to the thermal energy of ICM to be normalized. The thermal electron pressure $P_e(r)$ is often described with the help of the Generalized Navarro Frank White (GNFW) profile [18], which is a modified version of the earlier Navarro Frank White (NFW) profile [19]. The universal pressure profile for electrons, $\mathbb{P}_e(r)$, depends on four parameters: the normalizing factor P_0, the scale radius $r_p = R_{500}/c_{500}$ (here, the parameter $c_{500} = R_{500}/r_p$ characterizes the compactness degree of the central high-pressure region, and, according to numerical simulation results, $c_{500} \approx 4.2$ [10, 20]), and three power exponents a_p, b_p, and c_p, which determine the distribution slope in different spatial regions ($r < r_s$, $r \approx r_s$, and $r > r_s$, respectively):

$$\mathbb{P}_e(r) = \frac{P_0}{\left(\frac{r}{r_p}\right)^{c_p} \left[1 + \left(\frac{r}{r_p}\right)^{a_p}\right]^{\frac{b_p - c_p}{a_p}}}. \qquad (3)$$

In order to describe the electron pressure profile $P_e(r)$ in a particular GC, the universal pressure profile (3) has to be multiplied by a few normalizing factors characterizing this GC,

$$P_e(r) = \mathbb{P}_e(r)\, P_{500}\, F_{500}, \qquad (4)$$

where P_{500} is a characteristic pressure [18, 20], which can be determined knowing the GC mass and the

cosmological parameters,

$$P_{500} = 1.65 \times 10^{-3} E(z)^{8/3} \left(\frac{M_{500}}{3 \times 10^{14} h_{70}^{-1} M_\odot} \right)^{2/3} h_{70}^2,$$

$$(5)$$

whereas the factor F_{500} makes corrections related to the GC mass in accordance with self-similar models,

$$F_{500} = \left(\frac{M_{500}}{3 \times 10^{14} h_{70}^{-1} M_\odot} \right)^{0.12}.$$

$$(6)$$

Here, $H_0 = 100h$ km$/$(s Mpc), $h_{70} = h/0.70$, and $E(z) = H(z)/H(0)$ or $E^2(z) = \Omega_M(1 + z)^3 + \Omega_\Lambda$.

For an ICM with the mass fractions of hydrogen X, helium Y, and heavy elements $Z = 1 - X - Y$, the average molecular weights are $\mu_{\text{gas}} = 0.60$ and $\mu_e = 1.15$ if $Y = 0.27$ and $Z = 0.005$. Therefore, the pressure, density, and temperature of the ICM gas can be expressed in terms of the electron pressure and density in the ICM [10]:

$$P_{\text{gas}}(r) = \frac{\mu_e}{\mu_{\text{gas}}} P_e(r),$$

$$(7)$$

$$\rho_{\text{gas}}(r) = \frac{\mu_e}{\mu_{\text{gas}}} m_H n_e(r),$$

$$(8)$$

$$k_B T_{\text{gas}}(r) = \mu_{\text{gas}} m_H \frac{P_{\text{gas}}(r)}{\rho_{\text{gas}}(r)}.$$

$$(9)$$

The magnetic field distribution in the GCs reproduces the matter distribution [21, 22]. Based on the freezing-in conditions, the spatial distribution of the magnetic field, $B(r)$, can be represented as proportional to the density profile raised to a certain power exponent η_B,

$$B(r) = B_0 \left[\frac{n_e(r)}{n_{e,0}} \right]^{\eta_B}.$$

$$(10)$$

The normalization factor was chosen to equal $B_0 = 4.7$ μGs. This is a typical value for GCs, which was calculated for the Coma cluster on the basis of the data measured for the Faraday rotation effect [21]. The spatial-energy distributions $dN_i(E, r)/dE$ of nuclei (mainly protons, $i = p$) and electrons ($i = e_1$ for primary electrons and $i = e_2$ for secondary electrons formed at inelastic collisions) in the CRs in the ICM can be factorized as the product of the energy and spatial distributions,

$$\frac{dN_i(E, r)}{dE} = A_i f_i(E) \phi_i(r).$$

$$(11)$$

Relativistic protons and electrons in the ICM, being accelerated by shock waves inside the GCs, acquire a power-law energy distribution. In this work, the classical power law (PL) with exponential cut-off (EC) was used to describe the energy spectrum,

$$f_i(E) = A_i \left(\frac{E}{E_{0,i}} \right)^{-\alpha_i} \exp \left(-\frac{E}{E_{\text{cut},i}} \right),$$

$$(12)$$

where α_i is the spectral index, and the cut-off is made at the energies $E_{\text{cut},i}$ ($i = p, e_1$). The normalizing factor A_i is determined via the ratios between the CR energy U_{CR} and the thermal energy U_{th} inside the sphere of radius $r = R_{500}$,

$$X_{\text{cr},i,\text{th}} = \frac{U_{\text{CR},i}(R_{500})}{U_{\text{th}}(R_{500})}.$$

Typical values of those ratios are $X_{\text{cr,p,th}} \approx 0.02 \div 0.10$ and $X_{\text{cr,e,th}} \approx 0.0001 \div 0.001$. The spatial distribution of CRs inside the ICM is related to the gas distribution, and it can be approximated by the power-law dependence with the free parameter $\eta_{\text{CR},i}$,

$$\phi_i(r) = \left[\frac{n_e(r)}{n_e(0)} \right]^{\eta_{\text{CR},i}}.$$

$$(13)$$

It is also important to pay attention to such a key parameter as the cut-off radius R_{tr}, which is used to denote the physical boundaries of the area containing the entire GC volume, with the density vanishing outside. At this distance from the GC center, the thermodynamic parameters undergo a discontinuity. The latter is determined by the location of the accretion shock wave where the kinetic energy of the accretion flux is converted into the thermal energy of the gas decelerated by the shock wave [23]. The size of this region is determined by the characteristic radius $R_{\text{tr}} \approx 3R_{500}$.

3. Gamma and Neutrino Radiation of the A1656 Intracluster Medium

The parameters of the thermal and non-thermal radiation emitted by GCs are determined by the spatial distribution of matter (dark and baryon), magnetic fields, and CRs (the leptonic and hadronic components) inside the ICM. To find those distributions, observational data concerning the surface brightness distribution of thermal X-ray radiation, I_X, and the spectral distortion of the cosmic microwave background (CMWB) as a result of the Sunyaev–Zeldovich effect, $\Delta I/I$, are used [10]. The former is
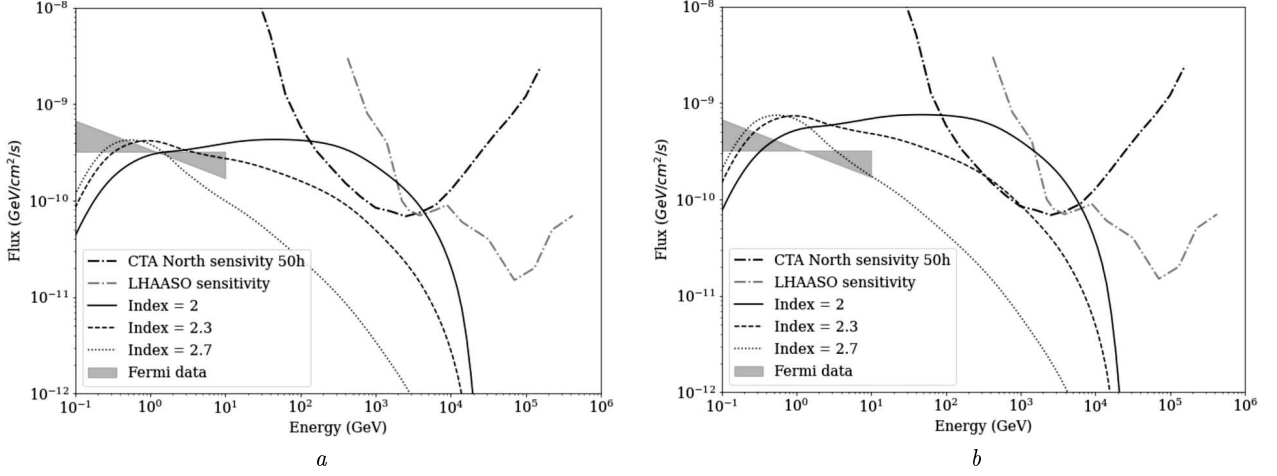
Fig. 1. Spectral flux of gamma radiation from A1656 for various values of spectral index for the distribution of $CRp \propto n_e(r)$. Below: for the CR distributions $CRp \propto n_e(r)$ (*a*) and $CRp \propto n_e(r)^2$ (*b*). See other parameters in Table

proportional to the product of the cooling function $\Lambda(T_e, Z)$ and the squared electron concentration n_e^2 integrated along the line of sight l,

$$I_X \propto \int n_e^2 \Lambda(T_e, Z) dl,$$

whereas the latter is proportional to the integral of the electron pressure P_e taken along the line of sight,

$$\Delta I / I \propto \int P_e dl.$$

The indicated data make it possible to solve the inverse problem, namely, to restore the spatial distributions of the temperature $T_e(r)$, electron concentration $n_e(r)$, partial pressure of electrons $P_e(r)$, and total pressure of baryonic gas $P_{\text{gas}}(r)$ inside the ICM. Using the formulas presented in the previous section, we can simulate the distributions of magnetic fields [Eq. (10)] and CRs [Eq. (13)] in the ICM. The recent work [24] contains new observational results on thermal X-ray radiation and the restoration of the thermodynamic plasma parameters of the ICM of A1656 that were obtained from observations of the new SRG/eROSITA X space X-ray mission.

Taking the available data into account, a set of parameters necessary for modeling gamma and neutrino radiation from the Coma GC making use of the MINOT software code has been formed (see Table). The absorption of gamma-ray flux owing to the interaction with intergalactic background radiation
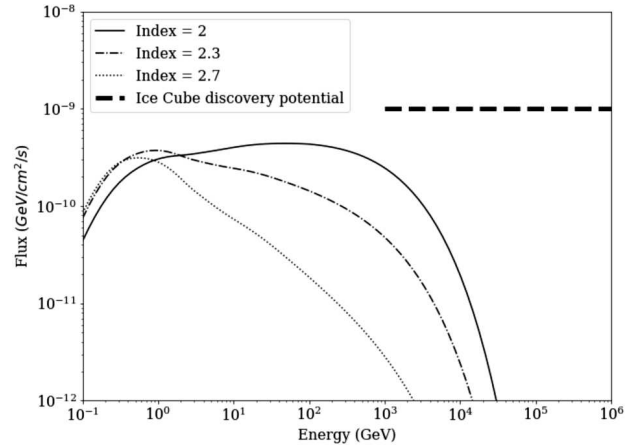

Fig. 2. Calculated neutrino flux for various values of spectral index. The thick dashed line demonstrates the IceCube 5σ detection potential in an energy interval of 1–1000 TeV [29]

[25] was made allowance for with the help of the Python software package *ebltable* [26].

At first, we calculated the expected spectra of gamma (Fig. 1) and neutrino (Fig. 2) radiation for physical models neglecting the contributions made by the AGN and the merging processes to the total CR stock. While comparing various models of CR distribution in the ICM, we simulated the gamma-ray flux using three values for the spectral index, $\alpha_p = 2$, 2.3, and 2.7 (see Fig. 1). The cases that are the most promising for CTA detection correspond to the hard CR spectrum (the spectral index $\alpha_p \approx 2$). (The sensitivity of the CTA experiment was taken from site [27],

**Model parameters
for gamma-ray emission of GC A1656**

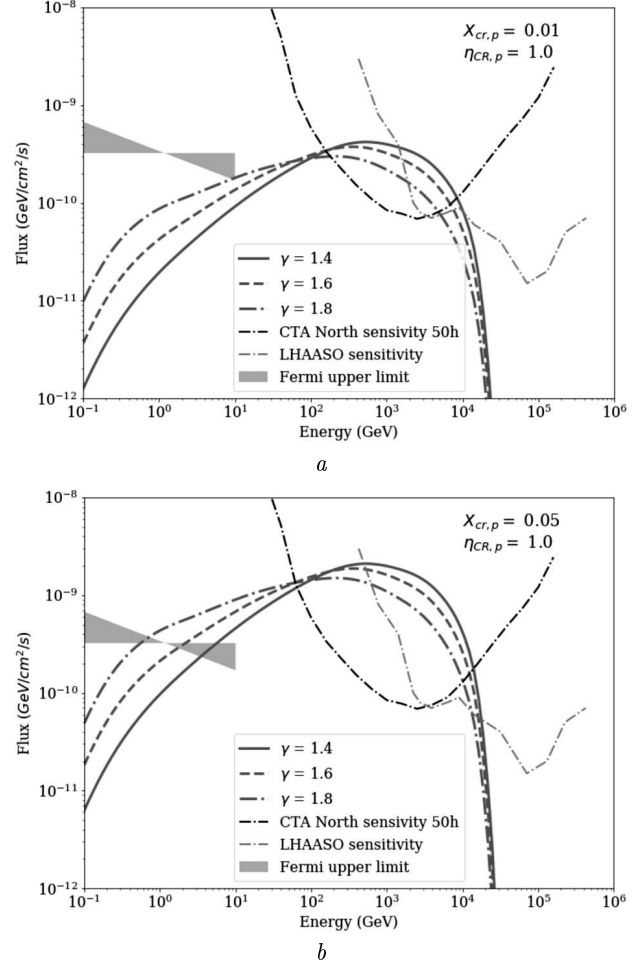| General parameters	Basic model (ICM contribution only)	Model with AGN contribution
z	0.0231	0.0231
M_{500} $[10^{14} M_\odot]$	6.13	6.13
R_{500} [kpc]	1310	1310
R_{trunc} [kpc]	3930	3930
Helium mass fraction	0.2735	0.2735
Metallicity	0.0153	0.0153
Abundance	0.3	0.3
Correction parameter		
b_{HSE}	0.2	0.2
Cosmic ray distribution model		
$X_{\mathrm{cr},p} = U_{cr,p}/U_{\mathrm{th}}$ inside R_{500}	0.02	0.01–0.05
$X_{\mathrm{cr},e1} = U_{cr,e1}/U_{\mathrm{th}}$ inside R_{500}	0.00002	0.00001–0.00005
$E_{p,\min}$ [GeV]	1.21	1.21
$E_{p,\mathrm{cut}}$ [TeV]	30	30
$E_{p,\max}$ [TeV]	10^6	10^6
Spectral index		
α_p (model)	2.3 (PL + EC)	1.8 (PL + EC)
$E_{e1,\min}$ [keV]	511	511
$E_{e1,\mathrm{break}}$ [GeV]	–	–
$E_{e1,\mathrm{cut}}$ [TeV]	–	–
$E_{e1,\max}$ [TeV]	10^{-2}	10^{-2}
Spectral index		
α_{e1} (model)	3.0 (PL)	3.0 (PL)
CR_p density distribution: $n_{\mathrm{CR},p}(r) \propto n_e(r)^{\eta_{\mathrm{CR},p}}$	$\eta_{\mathrm{CR},p} = 1.0$–2.0	$\eta_{\mathrm{CR},p} = 1.0$
CR_{e1} density distribution: $n_{\mathrm{CR},e}(r) \propto n_e(r)^{\eta_{\mathrm{CR},e}}$	$\eta_{\mathrm{CR},e} = 1.0$–2.0	$\eta_{\mathrm{CR},e} = 1.0$
Gas pressure distribution model		
P_0 [keV/cm^3]	0.022	0.022
a_p	1.8	1.8
c_p	0.0	0.0
r_p [kpc]	466.8	466.8
Gas density distribution model		
n_0 [cm^{-3}]	3.36×10^{-3}	3.36×10^{-3}
r_c [kpc]	310	310
β_{dens}	0.75	0.75
Magnetic field distribution model		
B_0 [[μGs]]	4.7	4.7
η_{B}	0.5	0.5

Fig. 3. Gamma-ray spectra for the AGN inside A1656 for the parameter values $X_{\mathrm{cr.p}} = 0.01$ (*a*) and 0.05 (*b*)

and the sensitivity of the LHAASO one from work [28].) At the same time, a twofold enhancement of the gamma-ray flux occurring owing to a more compact spatial distribution of CRs is observed only at low energies (not higher than tens of GeVs, Fig. 1). Therefore, it follows from Fig. 1 that the Coma cluster (A1656) can be detected in the TeV spectral interval using the CTA array only if the CR spectrum is hard. The calculated neutrino flux from A1656 is shown in Fig. 2 together with the observed IceCube potential at a statistical significance level of 5σ.

4. AGN Contribution to Gamma and Neutrino Radiation of A1656

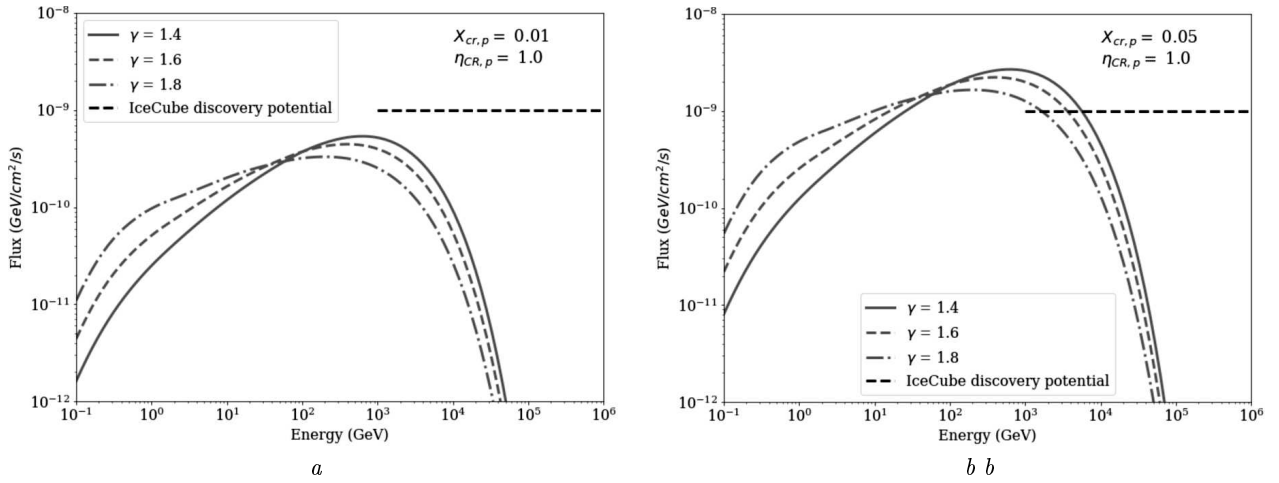We expect that the AGN in A1656 can substantially contribute to the total CR amount in the ICM of

Fig. 4. Neutrino spectra for the AGN inside A1656 for the parameter values $X_{cr,p} = 0.01$ (*a*) and 0.05 (*b*)

this GC. Taking into account the processes of active merging of two GCs associated with the NGC4839 group and A1656 [24], let us consider a model with a harder radiation spectrum, which is formed owing to the additional contribution to the total CR amount from the AGN and the merging processes. As a result of CR acceleration in AGN jets − in particular, owing to magnetic switching − the expected spectral index of such CRs will be hard with typical values $\alpha_p = 1.4 \div 1.8$ for strongly magnetized plasma [30]. The corresponding spectrum of gamma radiation from pp-collisions in CRs accelerated in the jets is depicted in Fig. 3 for three values of the spectral index, $\alpha_p = 1.4, 1.6,$ and 1.8.

The most promising for the CTA detection is the CR spectrum with the hardest spectral index ($\alpha_p = 1.4$ in our calculations). In Fig. 4, a neutrino flux calculated in the hard spectrum case is exhibited. One can see that in our model, IceCube can register neutrino events already if the CR energy fraction in the thermal ICM energy equals $X_{cr.p} \approx 0.05$. It is important to note that, unlike photons, neutrinos do not undergo energy losses due to their interaction with the CMWB at TeV energies: the neutrino spectrum, which reproduces the CR spectrum with the energy shift $E_\nu \approx 0.1 E_p$, is exponentially cut at energies $E_{\nu,\text{cut}} \approx 0.1 E_{p,\text{cut}} \approx 3$ TeV only due to the high-energy cut-off of the CR spectrum at $E_{p,\text{cut}} = 30$ TeV in the considered case (Figs. 2 and 4). For the CR spectrum with $E_{p,\text{cut}} = 300$ TeV, we have $E_{\nu,\text{cut}} \approx \approx 30$ TeV. At the same time, owing to $\gamma + \gamma \to e^+ + e^-$ annihilations, the path length of 10–100-TeV photons

equals $\lambda_{\gamma\gamma} \approx 200 \times (E_\gamma/10 \text{ TeV})^{-2}$ Mpc [24] and gives rise to an additional abrupt cut-off of the gamma radiation spectrum from the Coma GC (at a distance of about 100 Mpc) at energies of about 20 TeV (Figs.1 and 3). This fact confirms the prospects of neutrino studies of physical processes running in GCs.

5. Conclusions

Since the time of diffusive escape of CRs from GCs is long, the latter should be bright extragalactic sources of neutrinos and non-thermal gamma radiation. On the basis of current data obtained for thermal X-ray radiation and thermodynamic parameters of plasma inside the GC A1656 [13, 24], we simulated non-thermal gamma and neutrino radiation using the MINOT software [10]. The simulation of hadronic gamma radiation emitted from the Coma GC as a result of pp-collisions of CR protons with ICM plasma is consistent with *Fermi*-LAT observational data (100 MeV–300 GeV) at typical CR parameters; namely, the ratio between the CR energy and the plasma thermal energy $X_{cr,p} \approx 0.02$, the spectral index $\alpha_p = 2.3 \div 2.7$, and the spatial distribution of CRs traces the matter distribution [13] (see also Fig. 1). Additionally, a more compact spatial distribution of CRs insignificantly increases the spectral flux (by a factor of two for $\eta_{cr,p} = 2$). Owing to large values of the spectral index (they correspond to small values of the Mach number M for the shock waves at the fronts of which CRs accelerate), the spectral fluxes of TeV gamma radiation are insufficient

for reliable detection. The situation can be better for CRs with a hard spectrum, i.e., with small values of the spectral index, $\alpha_p \leq 2$ (Fig. 3). The hard CR spectrum is expected for the CR acceleration at the fronts of strong shock waves ($M \geq 10$, $\alpha_p \approx 2$) or at the switching of the magnetic field lines in the AGN jets ($\alpha_p < 2$) [7]. In GCs – in particular, the Coma GC – strong shock waves can accompany the processes of substructure merging, and jets are certainly present in the radio-loud AGNs inside GCs. Figure 3 demonstrates that CRs with a hard spectrum can provide a detectable spectral flux of TeV gamma radiation even at a relatively small fraction of CR energy, $X_{\mathrm{cr},p} \approx 0.01$.

To summarize, we would like to note that the simulation results obtained for the fluxes of non-thermal gamma radiation and neutrinos from the Coma GC testify to a real possibility of its registration with available (*Fermi*-LAT, LHAASO, Ice-Cube) and planned ground-based (CTA, IceCube-Gen2) detectors.

1. G.M. Voit. Tracing cosmic evolution with clusters of galaxies. *Rev. Mod. Phys.* **77**, 207 (2005).
2. V.Springel, C. Frenk, S. White. The large-scale structure of the Universe. *Nature* **440**, 1137 (2006).
3. S. Allen, A. Evrard, A. Mantz. Cosmological parameters from observations of galaxy clusters. *Ann. Rev. Astron. Astrophys.* **49**, 409 (2011).
4. V. Berezinsky, P. Blasi, V. Ptuskin. Clusters of galaxies as storage room for cosmic rays. *Astrophys. J.* **487**, 529 (1997).
5. J. Mohr, B. Mathiesen, A. Evrard. Properties of the intracluster medium in an ensemble of nearby galaxy clusters. *Astrophys. J.* **517**, 627 (1999).
6. C. Pfrommer, T. Enslin. Constraining the population of cosmic ray protons in cooling flow clusters with γ-ray and radio observations: Are radio mini-halos of hadronic origin? *Astron. Astrophys.* **413**, 17 (2004).
7. A. Pinzke, C. Pfrommer. Simulating the γ-ray emission from galaxy clusters: a universal cosmic ray spectrum and spatial distribution. *Mon. Not. R. Astron. Soc.* **409**, 449 (2010).
8. M. Ackermann, A. Ajello, A. Allafort *et al.* Search for cosmic-ray-induced gamma-ray emission in galaxy clusters. *Astrophys. J.* **787**, 18 (2014).
9. D. Wittor. On the challenges of cosmic-ray proton shock acceleration in the intracluster medium. *New Astron.* **85**, 101550 (2021).
10. R. Adam, H. Goksu, A. Leingartner-Goth *et al.* MINOT: Modeling the intracluster medium (non-)thermal content and observable prediction tools. *Astron. Astrophys.* **644**, A70 (2020).
11. Planck Collaboration *et al.* Planck 2015 results. XIII. Cosmological parameters. *Astron. Astrophys.* **594**, A13 (2016).
12. S.-Q. Xi, X.-Y. Wang, Y.-F. Liang *et al.* Detection of gamma-ray emission from the Coma cluster with Fermi Large Area Telescope and tentative evidence for an extended spatial structure. *Phys. Rev. D* **98**, 063006 (2018).
13. R. Adam, H. Goksu, S. Brown *et al.* γ-ray detection toward the Coma cluster with Fermi-LAT: Implications for the cosmic ray content in the hadronic scenario. *Astron. Astrophys.* **648**, A60 (2021).
14. S. Garrappa, S. Buson, Fermi-LAT Collaboration. Fermi-LAT gamma-ray observations of IceCube-200921A and detection of a new gamma-ray source, Fermi J1256.9 + 2630. *GRB Coordinates Network* **28481**, 1 (2020).
15. Planck Collaboration *et al.* Planck 2013 results. XX. Cosmology from Sunyaev–Zeldovich cluster counts. *Astron. Astrophys.* **571**, A20 (2014).
16. R. Piffaretti, R. Valdarnini. Total mass biases in X-ray galaxy clusters. *Astron. Astrophys.* **491**, 1 (2008).
17. A. Cavaliere, R. Fusco-Femiani. The distribution of hot gas in clusters of galaxies. *Astron. Astrophys.* **70**, 677 (1978).
18. D. Nagai, A.V. Kravtsov, A. Vikhlinin. Effects of galaxy formation on thermodynamics of the intracluster medium. *Astrophys. J.* **668**, 1 (2007).
19. J. Navarro, C. Frenk, S. White. The structure of cold dark matter halos. *Astrophys. J.* **462**, 563 (1996).
20. M. Arnaud, G.W. Pratt, R. Piffaretti *et al.* The universal galaxy cluster pressure profile from a representative sample of nearby systems (REXCESS) and the $Y_{\mathrm{SZ}} - M_{500}$ relation. *Astron. Astrophys.* **517**, A92 (2010).
21. A. Bonafede, L. Feretti, M. Murgia *et al.* The Coma cluster magnetic field from Faraday rotation measures. *Astron. Astrophys.* **513**, A30 (2010).
22. M. Murgia, F. Govoni, L. Feretti *et al.* Magnetic fields and Faraday rotation in clusters of galaxies. *Astron. Astrophys.* **424**, 2 (2004).
23. G. Hurier, R. Adam, U. Keshet. First detection of a virial shock with SZ data: implication for the mass accretion rate of Abell 2319. *Astron. Astrophys.* **622**, A136 (2019).
24. E. Churazov, I. Khabibullin, N. Lyskova *et al.* Tempestuous life beyond R_{500}: X-ray view on the Coma cluster with SRG/eROSITA. I. X-ray morphology, recent merger, and radio halo connection. *Astron. Astrophys.* **651**, A41 (2021).
25. E. Dwek, F. Krennrich. The extragalactic background light and the gamma-ray opacity of the universe. *Astropart. Phys.* **43**, 112 (2013).
26. https://github.com/me-manu/ebltable/.
27. https://www.cta-observatory.org/science/cta-performance/.
28. X. Bai, B.Y. Bi, X.J. Bi *et al.* The Large High Altitude Air Shower Observatory (LHAASO) Science White Paper – 2021 Edition. *arXiv:* 1905.02773 [astro-ph.HE] (2019).
29. Ice Cube Collaboration *et al.* Search for steady point-like sources in the astrophysical muon neutrino flux with 8 years of IceCube data. *Eur. Phys. J. C* **79**, 234 (2019).

30. G.R. Werner, D.A. Uzdensky, B. Cerutti *et al.* The extent of power-law energy spectra in collisionless relativistic magnetic reconnection in pair plasmas. *Astrophys. J. Lett.* **816**, L8 (2016).

Р.Б. Гнатик, В.В. Войцеховський

ГАММА- ТА НЕЙТРИННЕ
ВИПРОМІНЮВАННЯ СКУПЧЕННЯ
ГАЛАКТИК ВОЛОССЯ ВЕРОНІКИ (A1656)

Скупчення галактик (СГ) є найбільшими і наймасивніши-ми гравітаційно зв'язаними об'єктами у великомасштабній структурі Всесвіту. Через значні (порядку кеВ) температу-ри віріалізованого газу у внутрішньокластерному середови-щі (ВКС) та наявність космічних променів (КП) СГ є ефек-тивними джерелами теплового рентгенівського та нетепло-вого лептонного (синхротронного) випромінювання. При-скорені КП акумулюються в СГ, оскільки час дифузійного виходу КП із СГ перевищує вік Всесвіту. Однак нетепло-ве адронне гамма-випромінювання (головно, через протон-протонні зіткнення КП з тепловими протонами плазми ВКС та наступні розпади нейтральних піонів) від СГ ще не було надійно задетектоване. В цій роботі ми моделюємо очікуване нетеплове адронне гамма-випромінювання та по-тік нейтрино від СГ Волосся Вероніки (Coma cluster, A1656) та оцінюємо перспективи реєстрації цього випромінювання існуючими (*Fermi*-LAT, LHAASO, IceCube) та запланова-ними наземними (CTA, IceCube-Gen2) детекторами.

К л ю ч о в і   с л о в а: скупчення галактик, Скупчення Волос-ся Вероніки, космічні промені, гамма-випромінювання, ней-тринне випромінювання.